

---

This is an electronic reprint of the original article.  
This reprint may differ from the original in pagination and typographic detail.

Kocen, Rok; Gasik, Michael; Gantar, Ana; Novak, Saša

## Viscoelastic behaviour of hydrogel-based composites for tissue engineering under mechanical load

*Published in:*  
Biomedical Materials

*DOI:*  
[10.1088/1748-605X/aa5b00](https://doi.org/10.1088/1748-605X/aa5b00)

Published: 28/04/2017

*Document Version*  
Publisher's PDF, also known as Version of record

*Published under the following license:*  
CC BY

*Please cite the original version:*  
Kocen, R., Gasik, M., Gantar, A., & Novak, S. (2017). Viscoelastic behaviour of hydrogel-based composites for tissue engineering under mechanical load. *Biomedical Materials*, 12(2), Article 025004.  
<https://doi.org/10.1088/1748-605X/aa5b00>

---

This material is protected by copyright and other intellectual property rights, and duplication or sale of all or part of any of the repository collections is not permitted, except that material may be duplicated by you for your research use or educational purposes in electronic or print form. You must obtain permission for any other use. Electronic or print copies may not be offered, whether for sale or otherwise to anyone who is not an authorised user.

PAPER • OPEN ACCESS

# Viscoelastic behaviour of hydrogel-based composites for tissue engineering under mechanical load

To cite this article: Rok Kocen *et al* 2017 *Biomed. Mater.* **12** 025004

View the [article online](#) for updates and enhancements.

## Related content

- [Bioamine-crosslinked gellan gum hydrogel for neural tissue engineering](#)  
Janne T Koivisto, Tiina Joki, Jenny E Parraga et al.
- [Frequency-independent viscoelasticity of carbonyl iron particle suspensions under a magnetic field](#)  
Lei Shan, Wenpeng Jia, Ming Zhou et al.
- [Nanostructured Pluronic hydrogels as bioinks for 3D bioprinting](#)  
Michael Müller, Jana Becher, Matthias Schnabelrauch et al.

## Recent citations

- [Understanding biomaterial-tissue interface quality: combined in vitro evaluation](#)  
Michael Gasik

# Biomedical Materials



## PAPER

# Viscoelastic behaviour of hydrogel-based composites for tissue engineering under mechanical load

### OPEN ACCESS

#### RECEIVED

5 November 2016

#### REVISED

25 December 2016

#### ACCEPTED FOR PUBLICATION

20 January 2017

#### PUBLISHED

6 March 2017

Original content from this work may be used under the terms of the [Creative Commons Attribution 3.0 licence](#).

Any further distribution of this work must maintain attribution to the author(s) and the title of the work, journal citation and DOI.



Rok Kocen<sup>1,2</sup>, Michael Gasik<sup>3</sup>, Ana Gantar<sup>1</sup> and Saša Novak<sup>1,4</sup>

<sup>1</sup> Department for Nanostructured Materials, Jožef Stefan Institute, Jamova cesta 39, 1000 Ljubljana, Slovenia

<sup>2</sup> Jožef Stefan International Postgraduate School, Jamova cesta 39, 1000 Ljubljana, Slovenia

<sup>3</sup> School of Chemical Engineering, Aalto University Foundation, Vuorimiehentie 2K, FI-00076 Aalto, Finland

<sup>4</sup> Author to whom any correspondence should be addressed.

E-mail: [sasa.novak@ijs.si](mailto:sasa.novak@ijs.si)

**Keywords:** hydrogel, rheology, gellan gum, bioactive glass, mechanical properties

## Abstract

Along with biocompatibility, bioinductivity and appropriate biodegradation, mechanical properties are also of crucial importance for tissue engineering scaffolds. Hydrogels, such as gellan gum (GG), are usually soft materials, which may benefit from the incorporation of inorganic particles, e.g. bioactive glass, not only due to the acquired bioactivity, but also due to improved mechanical properties. They exhibit complex viscoelastic properties, which can be evaluated in various ways. In this work, to reliably evaluate the effect of the bioactive glass (BAG) addition on viscoelastic properties of the composite hydrogel, we employed and compared the three most commonly used techniques, analyzing their advantages and limitations: monotonic uniaxial unconfined compression, small amplitude oscillatory shear (SAOS) rheology and dynamic mechanical analysis (DMA). Creep and small amplitude dynamic strain-controlled tests in DMA are suggested as the best ways for the characterization of mechanical properties of hydrogel composites, whereas the SAOS rheology is more useful for studying the hydrogel's processing kinetics, as it does not induce volumetric changes even at very high strains. Overall, the results confirmed a beneficial effect of BAG (nano)particles on the elastic modulus of the GG–BAG composite hydrogel. The Young's modulus of  $6.6 \pm 0.8$  kPa for the GG hydrogel increased by two orders of magnitude after the addition of 2 wt.% BAG particles (500–800 kPa).

## 1. Introduction

Medical applications of hydrogels as scaffold materials were extended for various tissue engineering applications [1–3]. Hydrogels can provide a suitable environment for the cells, meaning that they could be made biocompatible, biodegradable and with tuneable biomechanical properties. For bone tissue engineering scaffolds, it is known that hydroxyapatite (HA) and bioactive glass (BAG) have an ability to promote osteogenesis [4], but they are rather brittle and with limited strain compliance. Therefore, there is an interest in composites of hydrogels with HA or BAG particles for simultaneous tuning of their bioactive and biomechanical properties [5, 6].

Suitable mechanical properties of scaffolds are very important to provide direct support to the

surrounding tissue (especially in load-bearing applications) and also to provide a proper microenvironment for the cells. It has been suggested that the stiffness of the scaffold (substrate) and stresses generated from the cell–substrate strains substantially affect a cell's fate, especially for stem cell differentiation [7, 8]. In a recent study [9] it was shown that not only the stiffness but also relaxation and retardation times affect the fate of mesenchymal stem cells. Most of the tissues do not exhibit linear elasticity due to their main constituents (cells, extracellular matrices, structural proteins and water). Therefore, the viscoelastic behavior is one of the key parameters to be addressed in such studies [10]. Even for 'hard' tissues, like bone [11], viscoelastic properties are significant, especially at low strain rates and within the physiological frequency ranges. Therefore, to know how well the scaffold material resembles

the tissue being regenerated, their time and/or frequency dependent mechanical properties have to be evaluated in sufficient detail.

One of the most cited scaffold material properties in the literature is Young's (elastic) modulus, even when material behavior is known to be far from an elastic or pseudo-elastic mechanical response. Hydrogels on their own are complex hydrophilic polymer networks containing a large amount of water (up to 98%), which results in complex viscoelastic behavior. Sometimes they are even called poro-viscoelastic [12–14], counting apparent porosity as a fluid-filled fraction of specimen volume. Whereas for pure hydrogels some theoretical considerations can be employed to justify certain viscoelastic models and, respectively, testing procedures, for composite hydrogels containing HA or BAG particles this is not straightforward.

In this study, we employed and compared three techniques to analyze viscoelastic properties of the BAG-particle reinforced GG hydrogel and discussed their ability to describe the complex system. Monotonic uniaxial unconfined compression (UC) and small amplitude oscillatory compression (DMA) were performed on pre-gelled composites. Small amplitude oscillatory shear was carried out on composite samples, which were gelled in the rheometer. We evaluated the advantages and drawbacks of each technique in relation to the field of hydrogel-based composite materials for tissue engineering scaffold materials. We also paid attention to the versatility of the techniques such as ease of specimen handling, potential risks, and eventual hardware limitations. This study might serve as a guideline for choosing the most appropriate technique to characterize mechanical properties of a hydrogel-based scaffold material or as a tool for comparing the results of mechanical properties obtained by different techniques.

## 2. Material and methods

### 2.1. Sample preparation

Hydrogel samples were prepared from a polysaccharide gellan gum (GG) powder, which was dissolved in ultrapure water (MilliQ) preheated to 90 °C under constant stirring to a final concentration of 2.0 wt.% of GG. Sodium-free BAG powder (70 wt.% SiO<sub>2</sub>, 30 wt.% CaO) was synthesized using a sol-gel technique [15]. The BAG particles have an approximate size of 100 nm and are clustered to ~10 μm large agglomerates [6]. The GG–BAG hydrogel composites were prepared by admixing up to 8.0 wt.% of BAG powder into a hot solution of GG (see table 1) and sonicating with a high power sonicator (Hielscher UP400S, Germany) to disperse and de-agglomerate the BAG particles. The amount of BAG particles added to the GG hydrogel was based on our previous work [6]. The largest addition of BAG (8 wt. %) was limited by the increased gelation temperature that limits the ability of mixing

**Table 1.** Compositions of the examined hydrogel-based composites.

Sample	BAG (wt.%)	GG (wt.%)	Water (wt.%)
H0	0	2	98
H1	2	2	96
H2	4	2	94
H3	6	2	92
H4	8	2	90

and pouring the samples into the desired shape. Until this point, the sample was kept at 90 °C.

For rheological tests, this suspension was directly poured onto the measuring fixture, which was preheated to 90 °C, where it was allowed to gel during a measurement. For compression and DMA tests, the samples were prepared by pouring the hot GG–BAG suspension into a preheated Petri dish, which was then taken off the heater. After cooling down to room temperature, the suspension gelled, and the samples were cut out using a punch with 6 mm or 12 mm diameter. Samples were stored in ultrapure water in order to avoid drying. In these experiments we avoided the use of phosphate-buffered saline as it contains ions that could affect the final mechanical properties by crosslinking the polymer, and extra osmotic effects.

For correct analysis using various measuring principles and types of deformation, it is highly important to maintain a constant amount of water within the hydrogel-based samples having different geometries. Due to the technical limitations of specific techniques, no single solution is available. Specimens cannot be left exposed to air during all the measurements, since during SAOS and DMA they would dry up, causing improper changes in mechanical properties. In SAOS, submerging the samples in water would cause degradation at the circumference, while covering the samples with paraffin oil is not a convenient method for the other two measuring techniques. Therefore, we accommodated the way to maintain the samples unchanged during the measurement to each technique.

### 2.2. Monotonic uniaxial unconfined compression

Samples of  $11.9 \pm 0.1$  mm diameter and  $11.5 \pm 0.6$  mm height were tested in uniaxial unconfined compression at room temperature (22 °C), with a universal testing machine (Galdabini Quasar 50, Italy), using 100 N load cell. The samples were not submerged in water during the experiments since during the compression water was coming out of the sample, keeping the surface of the sample wet. The loading rate of compression was  $0.2 \text{ mm min}^{-1}$ , equivalent to a strain rate of the order of  $\sim 3 \cdot 10^{-4} \text{ s}^{-1}$  [16]. The tangent Young's modulus (E) was calculated from the initial linear part of the slope of the stress–strain curve, i.e. assuming the initial (instant) elastic behavior of the

material [17]. The Young's modulus for each composition was an average of five measured samples.

### 2.3. Small amplitude oscillatory shear (SAOS) rheology

Rheological measurements were performed in a rheometer (AntonPaar MCR 301, Austria) using a 50 mm cone and plate fixture, with a cone angle of  $1^\circ$ . The sample holder was preheated to  $90^\circ\text{C}$  and the exact amount of the sample in the form of a solution/suspension was pipetted and dropped onto the fixture. This assures a good contact between the sample and the fixture [18]. To prevent evaporation of water from the sample, paraffin oil was poured around the perimeter of the sample, and the insulating chamber was closed. The samples were visually checked that there was no mixing of the sample with the paraffin oil.

The specimens were cooled down to  $25^\circ\text{C}$  at a rate of  $0.5\text{ K min}^{-1}$  [19], during which viscoelastic properties were measured. During this temperature sweep, gelation was observed. The temperature of gelation was defined by the highest slope of the  $G'$ , although there was also a substantial difference in the temperature range of gelation. To determine the linear viscoelastic region of hydrogels, separate strain sweep tests were made. Based on these results, a common strain value was chosen and later used to record viscoelastic properties during cooling, and frequency sweeps. Each sample was used for a strain sweep test in a strain-controlled mode at the end, to ensure that all the measurements were done in the linear region.

### 2.4. Dynamic mechanical analysis (DMA)

Dynamic mechanical analysis was carried out using DMA242C (Netzsch Gerätebau, Germany). Samples of  $5.9 \pm 0.1\text{ mm}$  diameter and  $5 \pm 0.4\text{ mm}$  height were used since the maximum height was limited by the DMA diameter compression sample holder. The sample's aspect ratio was kept the same as with uniaxial unconfined compression to ensure a similar loading mode. To prevent evaporation of water from the sample's surface, all the samples were submerged in deionised water during measurements at  $25^\circ\text{C}$ . Strain sweep tests were made to determine the linear viscoelastic region of deformation, by deforming from  $1\ \mu\text{m}$  to  $20\ \mu\text{m}$  amplitudes with steps of  $1\ \mu\text{m}$  at  $1\text{ Hz}$  frequency, resulting in  $0.6\text{--}0.7\%$  maximum compressive deformation. Once the strain sweeps were completed, frequency sweep tests from  $100$  to  $0.1\text{ Hz}$  were performed in the linear viscoelastic region. All strain and frequency sweeps have been performed with a proportional factor (PF) of  $1.1$ , meaning that the  $0.1$  of the applied force amplitude was always kept at the sample to ensure contact between the sample and the upper compression plate. In addition, some creep measurements were done at various forces (from  $0.1$  to  $1.2\text{ N}$ ) and for all compositions.

## 3. Results and discussion

The macroscopic appearance of the hydrogel-based composite H1, containing  $2\text{ wt. \%}$  of BAG nanoparticle hydrogel is presented in figure 1(a), while the figures 1(b) and (c) illustrate the microstructure of the freeze-dried sample at two magnifications. It is evident that  $\sim 10\ \mu\text{m}$  large agglomerates of BAG particles (with an average size of  $200\text{ nm}$ ) are embedded within the GG struts and are homogeneously distributed within the composite. It has to be mentioned, however, that although such images are frequently used to illustrate the architecture of hydrogel-based scaffold materials, the observed pores are only characteristics of the freeze-dried material and therefore the image does not adequately describe the microstructure of the hydrogel in its functional form.

### 3.1. Monotonic uniaxial unconfined compression

To reduce the effect of viscous dissipation, quasi-static unconfined compression tests [16] were performed at very a low strain rate ( $\sim 0.3\text{ millistrains s}^{-1}$ ). However, even at this rate, a non-linear response of hydrogel composites can already be seen at small deformations (figure 2(a)). The inelastic contributions cannot be easily separated with this technique, neither is effect of viscoelasticity at small strains (near linear deformation region) possible to evaluate. Application of higher strain rates does not allow separate effects of non-linearity and viscoelasticity. Consequently, this method, despite its simplicity, cannot be used for characterization of viscoelasticity in the non-linear deformation region.

A significant difference between the stress-strain curves for the samples with different composition is evident from figure 2(a). In quantitative metrics, the 'quasi'-static Young's modulus of the GG sample without BAG addition (H0) measured in compression is  $6.6 \pm 0.8\text{ kPa}$  (figure 2(b)), clearly rising by two orders of magnitude after the addition of BAG particles ( $500\text{--}800\text{ kPa}$ ). Such a huge increase is presumably caused by  $\text{Ca}^{2+}$  ions released from BAG, acting as cross-linkers of double helices that form the GG network [19]. Further increasing the amount of BAG in composite samples (specimens from H1 to H3) does not significantly change the tangent Young's modulus, and the stress-strain curve does not show any specific trend of reinforcement at higher strains. This suggests that at  $2\text{ wt. \%}$  of BAG in the composite samples, maximum cross-linking density, responsible for mechanical stiffness, is already reached.

Further observation of the stress-strain behaviour revealed that even at deformations  $>5\%$  there is also no visible 'yield point' or point of destruction of the hydrogel network (not shown). The polymer network is being destroyed gradually, which could sometimes be observed visually with samples containing high BAG content. At large deformations outflow of water

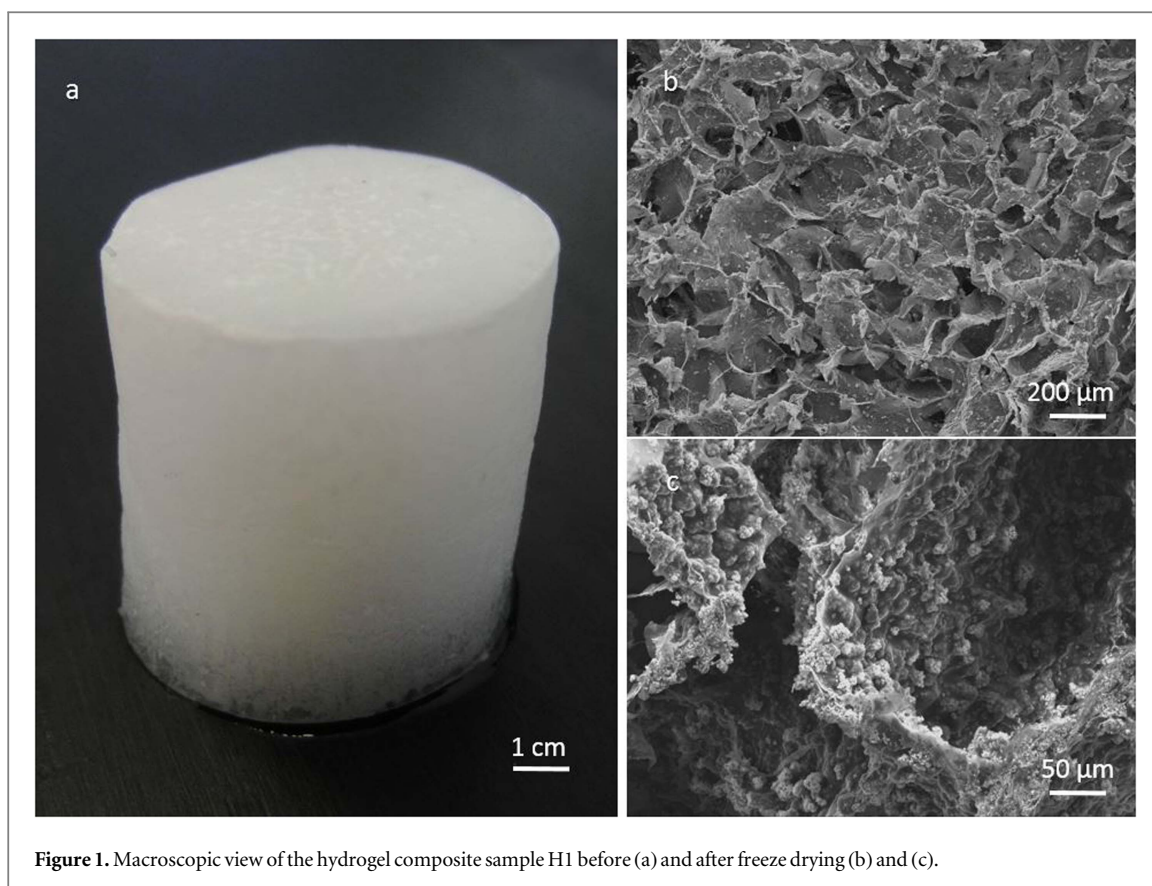


**Figure 1.** Macroscopic view of the hydrogel composite sample H1 before (a) and after freeze drying (b) and (c).

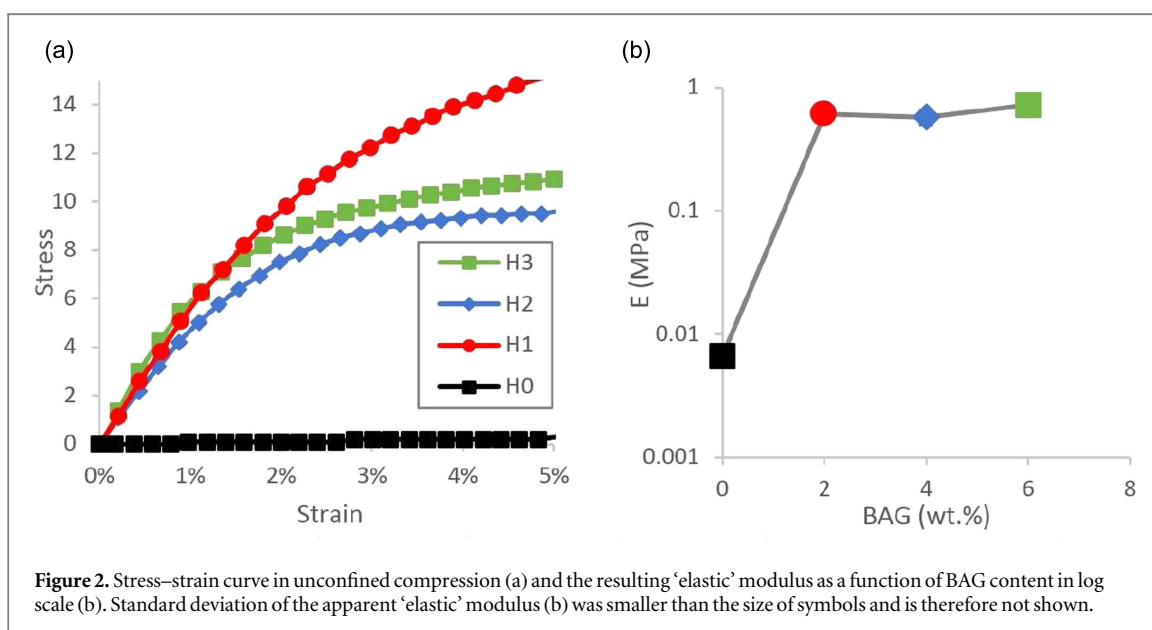


**Figure 2.** Stress–strain curve in unconfined compression (a) and the resulting ‘elastic’ modulus as a function of BAG content in log scale (b). Standard deviation of the apparent ‘elastic’ modulus (b) was smaller than the size of symbols and is therefore not shown.

of the samples was observed. Because the sample’s hydrogel matrix is transparent along with water on the surface, it is not possible to observe any cracks that might appear.

### 3.2. Small amplitude oscillatory shear (SAOS) rheology

To determine the linear viscoelastic region, preliminary strain sweeps of gelled samples were done from 0.01 to 100% torsion shear strain. The frequency of

oscillation was set to  $1.59 \text{ Hz}$  ( $10 \text{ rad s}^{-1}$ ). These tests showed that a rather small shear strain below 0.1% should be used during cooling and for frequency sweeps, to stay in the linear viscoelastic region and not to destroy the network.

Figure 3 shows measured viscoelastic properties of the samples during gelation. At the beginning (at  $90^\circ\text{C}$ ), all samples show a low modulus, as the samples are still in the form of a solution/suspension and have not yet formed a solid hydrogel network. However,

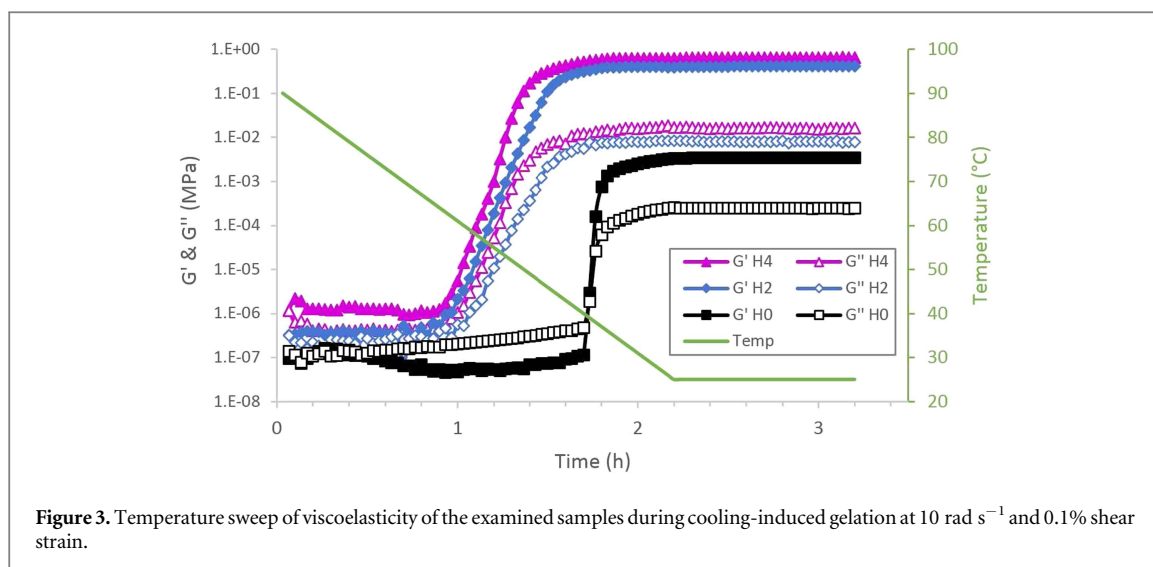


**Figure 3.** Temperature sweep of viscoelasticity of the examined samples during cooling-induced gelation at  $10 \text{ rad s}^{-1}$  and 0.1% shear strain.

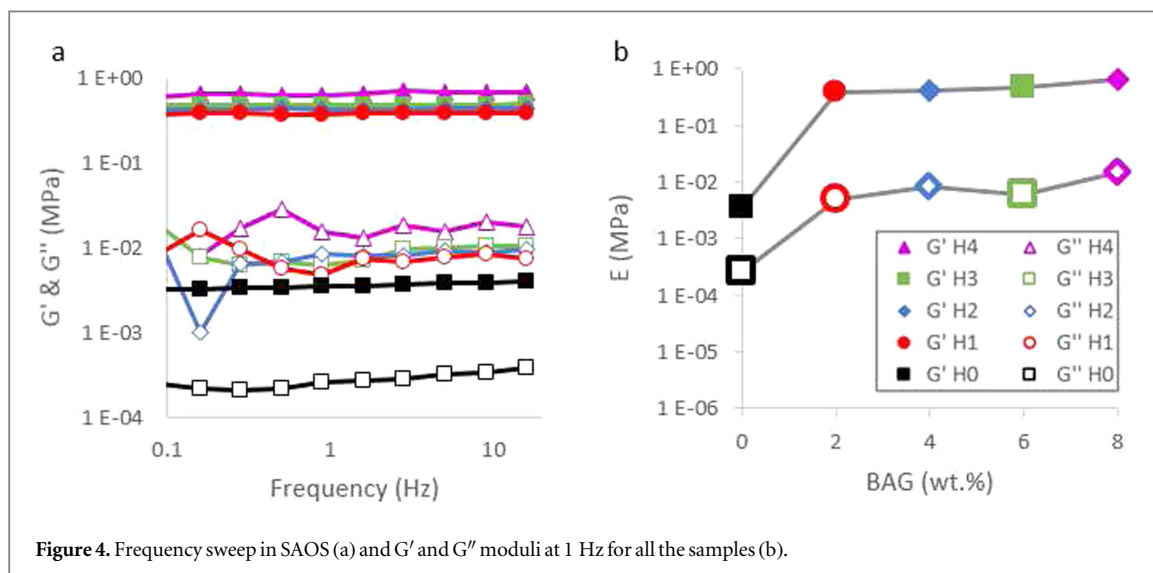


**Figure 4.** Frequency sweep in SAOS (a) and  $G'$  and  $G''$  moduli at 1 Hz for all the samples (b).

there is already a visible difference between different compositions of the composite hydrogel samples: BAG addition clearly increases shear moduli (both real  $G'$  and imaginary  $G''$ , also with the fact that  $G' > G''$ ). This implies that the introduction of BAG particles not only physically increases the viscosity of the GG solution, but also forms a weak network i.e. ‘weak gel’, as suggested by Gulrez *et al* [20]. This is caused by  $\text{Ca}^{2+}$  ions that increase the attraction forces between molecules of GG [21], and start to form a weak network of polymer chains. At this point, the material can still flow if subjected to higher strains that break the polymer network. This breakage occurs by the destruction of intermolecular bonds and not by breaking the polymer molecules. Therefore, when the outside forces are removed, and shear rate in the solution/suspension diminishes, the polymer network will again rearrange and form a weak gel. This means a weak gel could be poured into any shape without risk of affecting its molecular structure and the final mechanical properties.

Another difference observed in the properties when changing the amount of BAG is the increase of the gelation temperature with different amounts of BAG content (figure 3). The H0 sample gels (by cooling) around  $40^\circ\text{C}$ , and the increase of modulus is very rapid (square symbols). With the addition of BAG, the gelation starts at higher temperatures (onset  $60^\circ\text{C}$ – $70^\circ\text{C}$ ) with slower kinetics. This implies a change in the formation of the polymer network with the assistance of  $\text{Ca}^{2+}$  ions [19]. This means that even at a higher temperature, GG molecules have an attraction force high enough to form double helices i.e. forming a strong hydrogel network [20].

All gelled samples have approximate  $G'/G'' \sim 10$  and a little frequency dependence (figure 4(a)), which is usually an indicator of a self-standing elastic gel i.e. strong gel. The shear modulus of the gelled hydrogel also increases with increasing amount of BAG. As with the results of uniaxial compression, the most significant increase of moduli is observed after addition of 2 wt.% of BAG in GG, while no increase in shear modulus was observed by larger BAG additions (figure 4(b)).

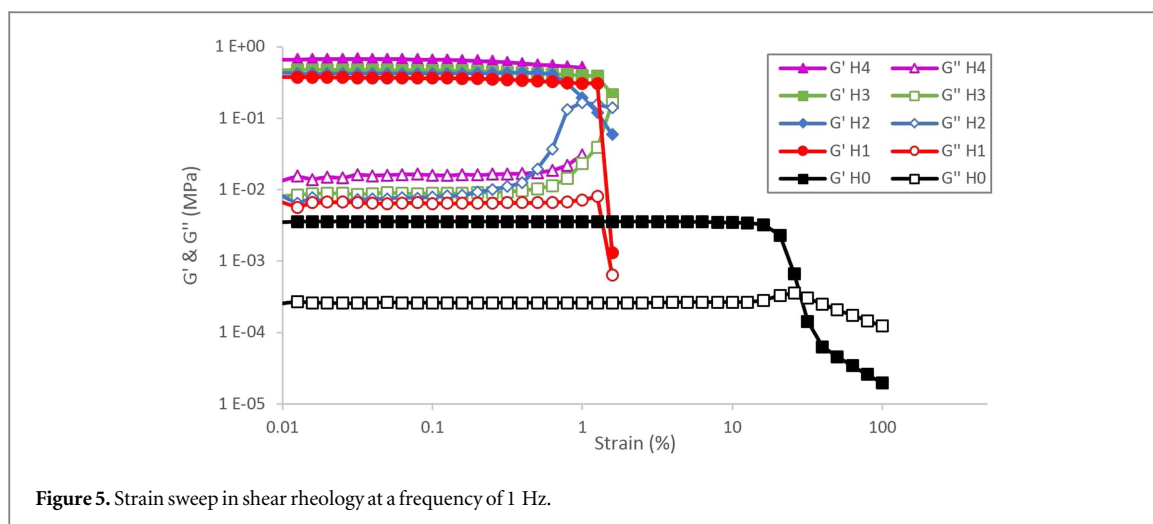


Figure 5. Strain sweep in shear rheology at a frequency of 1 Hz.

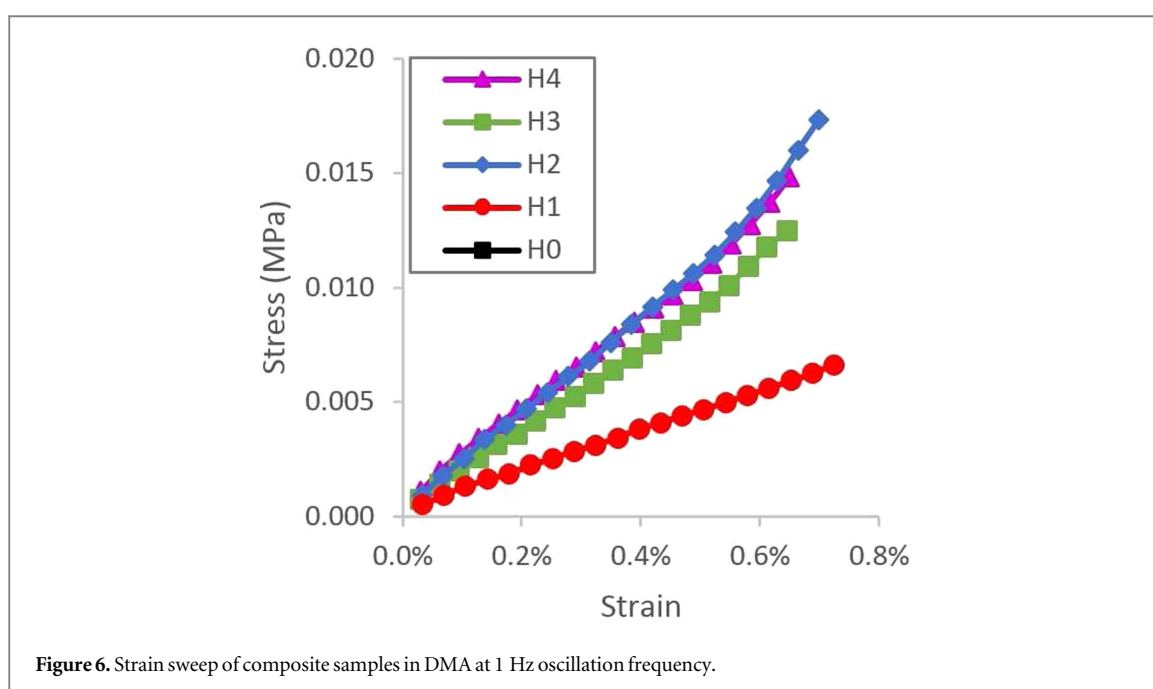


Figure 6. Strain sweep of composite samples in DMA at 1 Hz oscillation frequency.

As presented in figure 5, the range of linear behavior of the examined samples changed significantly with the addition of BAG in the GG hydrogel. The hydrogel without BAG (H0) shows linear region up to  $\sim 10\%$  of shear strain, leading to the hydrogel network destruction at higher strains. Once BAG is added, the linear viscoelastic region decreases to 0.3–1.0% only. However, again a further increase of BAG in composite samples (H1–H4) does not seem to affect linear viscoelastic region significantly. This confirms that all previous measurements at 0.1% strain deformation (frequency sweeps, measuring viscoelastic properties during cooling of the sample) were performed within the linear viscoelastic region.

### 3.3. Dynamic mechanical analysis (DMA)

The sample H0 (GG hydrogel without BAG) was found to be too weak for reliable measurement in the strain sweep mode. Due to non-controllable creeping

deformation upon contact with the sample holder, instability of the initial contact position appeared. BAG-reinforced hydrogels, on the contrary, were stable enough to carry out the measurements. Looking at figure 6, the H1 sample showed nearly linear deformation in the whole measured strain region. However, the rest of composites deviated somewhat from linearity at strain exceeding  $\sim 0.5\%$  (14–15  $\mu\text{m}$  axial deformation). Because of this, the following frequency sweeps were all done at 10  $\mu\text{m}$  deformation amplitude, to measure the samples in the linear viscoelastic region. This linear viscoelastic range is in excellent agreement with the linear viscoelastic range of oscillatory shear measurements (see figure 5).

Frequency sweep tests of the examined samples (H0–H4) have shown expected frequency dependence of a strong gel (figure 7(a)). Apparent storage modulus ( $E'$ ) does not significantly change with frequency, which is again analogous to the shear modulus ( $G'$ )

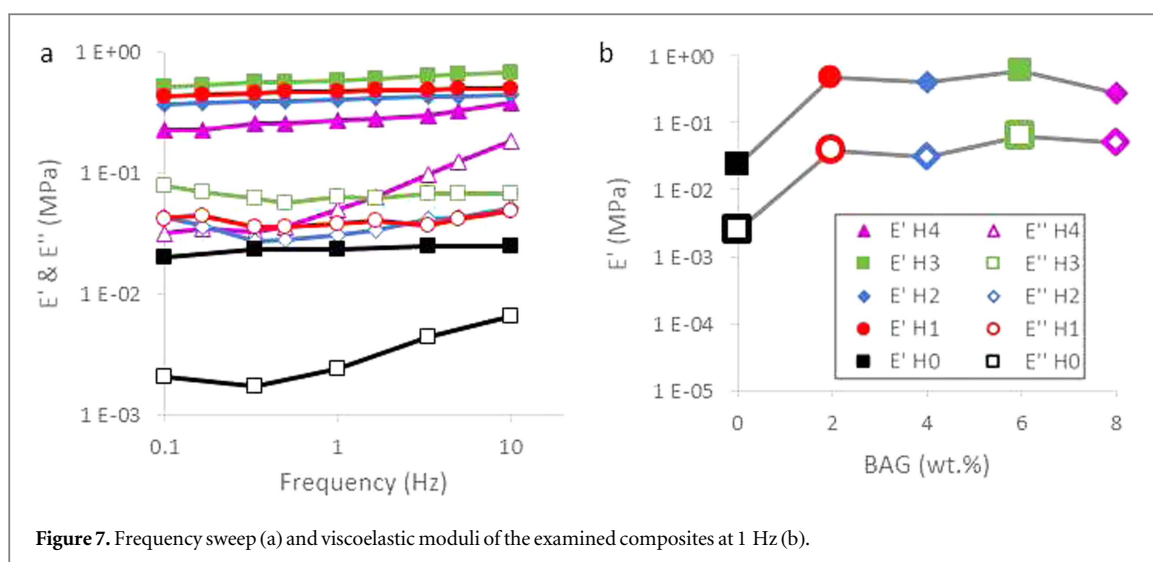


Figure 7. Frequency sweep (a) and viscoelastic moduli of the examined composites at 1 Hz (b).

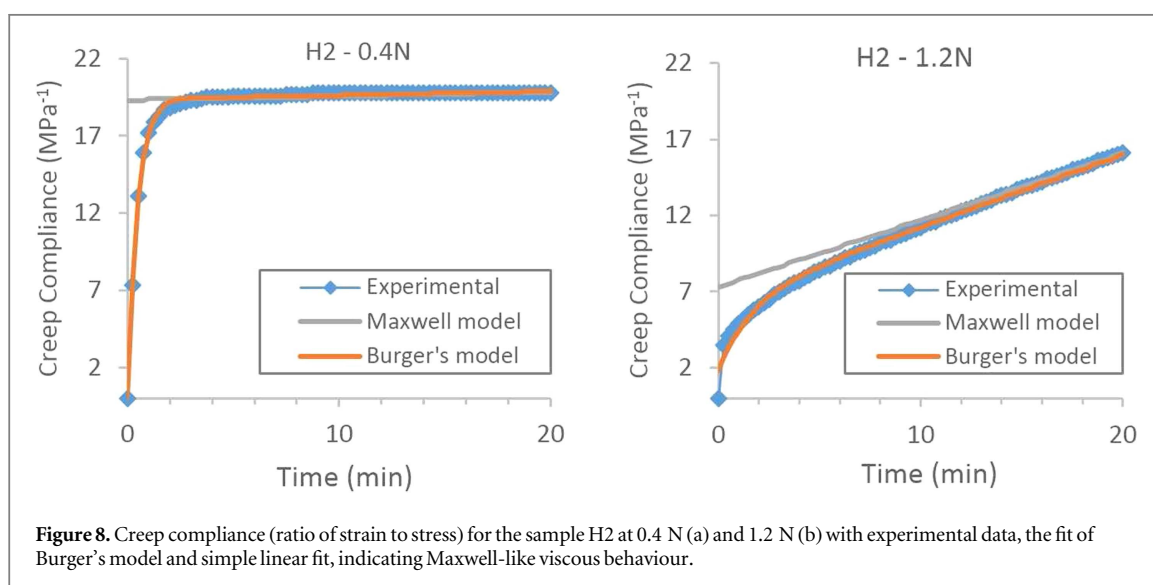


Figure 8. Creep compliance (ratio of strain to stress) for the sample H2 at 0.4 N (a) and 1.2 N (b) with experimental data, the fit of Burger's model and simple linear fit, indicating Maxwell-like viscous behaviour.

behavior obtained in SAOS experiments (figure 4(a)). Loss compression modulus ( $E''$ ) for all samples is approximately one order of magnitude lower than  $E'$ , which implies the behavior of a strong gel. As for 1 Hz frequency, a significant increase in both  $E'$  and  $E''$  is observed (figure 7(b)) for composite samples (H1–H4) in comparison with pure hydrogel (H0), whereas a minor difference is seen between the composite samples themselves.

The DMA device also allows for carrying out creep experiments in similar conditions to the frequency sweep. To compare the results of creep experiments for different samples at different creep forces, in figure 8 the experimental data for the sample H2 were fitted to constitutive models of linear viscoelasticity, i.e. Burger's model and Maxwell model. As evident, Burger's model fits very well to the experimental data at 0.4 and 1.2 N (figures 8(a) and (b), respectively), while Maxwell's model deviates in the initial creep region.

The fitting of the data with Burger's model (figure 9) was performed using a Matlab script with the

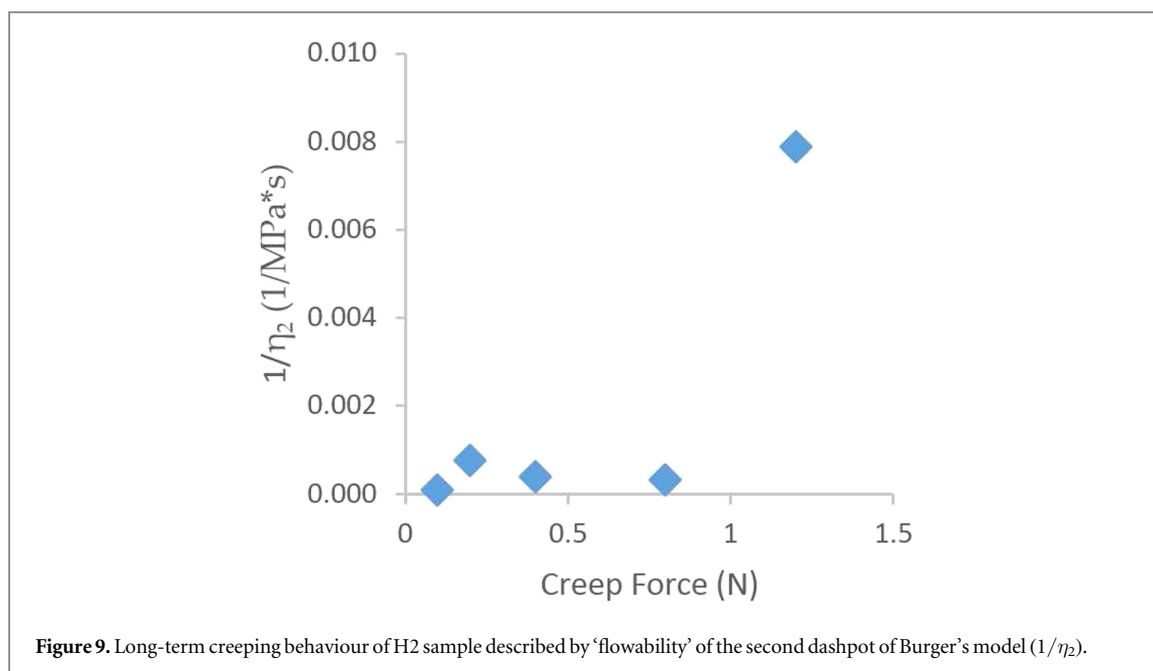
least squares method using the following equation (1):

$$D = t/\eta_2 + 1/E_1 \cdot (1 - \exp(-t/\tau_1)) + 1/E_2 \quad (1)$$

Constitutive equation of Burger's model was fitted to experimental creep compliance  $D$ , which is a ratio of strain and stress ( $D = \varepsilon/\sigma_0$ ). Here the parameter  $E_2$  ('Maxwell modulus') is proportional to the initial instantaneous deformation of the sample at the applied force. Elastic spring with modulus  $E_1$  and a dashpot with viscosity  $\eta_1$  in the parallel present a time-dependent response in creep, known as a Kelvin–Voigt model. This Kelvin–Voigt part of Burger's model has a characteristic retardation time  $\tau_1 = \eta_1/E_1$  that represents the time at which the sample deforms to 63% of its final deformation while excluding long-term creeping, expressed by 'Maxwell viscosity' of the dashpot  $\eta_2$ . The force applied was converted into the Lagrange stress  $\sigma = F/A_0$  for original cross-section of the specimen and the axial deformation was converted into true strain:

$$\varepsilon = \ln(1 + \Delta L/L_0) \quad (2)$$

While Burger's model was able to describe the response of all the examined samples, some of its



limitations need to be addressed. It is notable that due to sudden application of the creep force in a DMA method, the sensor is subjected to instant offset changes, which need to be re-compensated to correctly exclude the response of the sample holder, measuring electronics and the system hardware. Different DMA machines apply various algorithms to return the sensor origin to nearly zero offset range, which is normally a few micrometers depending on the resolution range set. Therefore, the very first part of the creep curve cannot be fully used for fitting unless the offset contribution is properly subtracted. Hence, the fitted  $E_2$  spring in Burger’s model does not solely depend on the response of the material, but also on the response of the DMA device and loading rate.

A more useful parameter is the reverse of Burger’s model dashpot viscosity ( $\eta_2$ ) or ‘flowability’ ( $1/\eta_2$ ). The effect of this parameter is clearly seen in figure 9, where the sample at a higher creep force ( $F = 1.2$  N) does not reach a steady state creep compliance in the same period. This ‘flowability’ of Burger’s model can be summed up for the H2 sample as a function of the creep force as shown in figure 8. Despite some scattering of the fitted parameter at lower forces, there is a clear increase of ‘flowability’ for the experiment at 1.2 N. This means that failure of the gelled network has occurred, resulting in more fluid-like behavior.

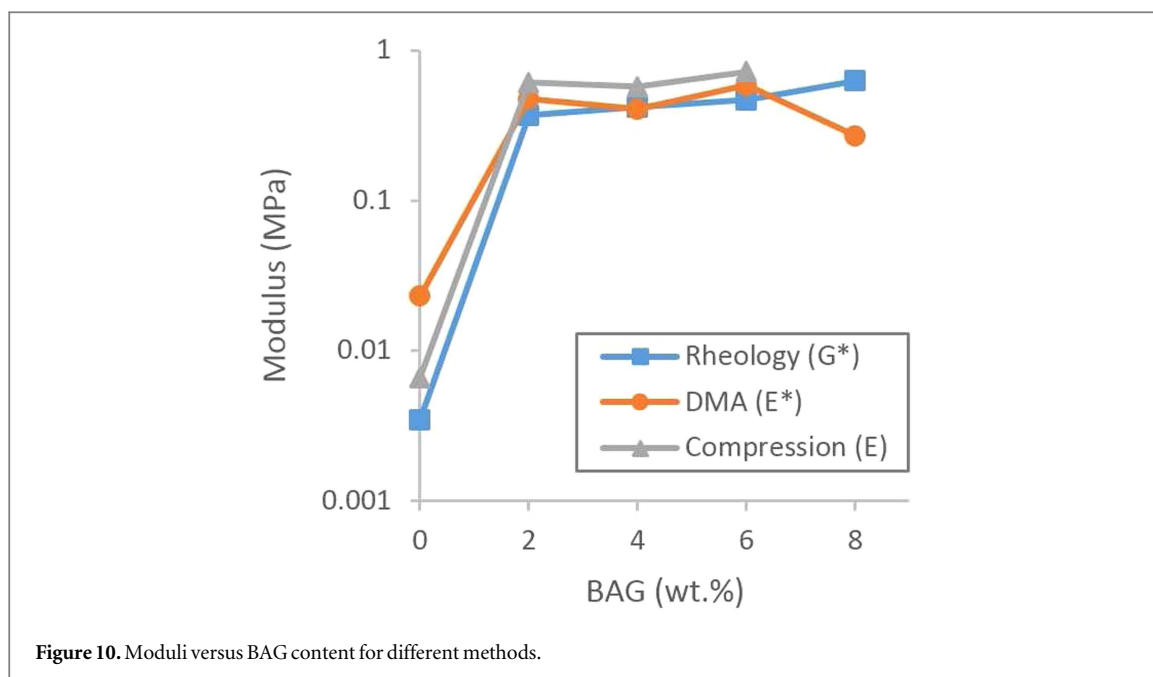
In addition, the results of the initial part of the creep data have rather a larger scatter due to establishing a proper contact between the specimen and the sensor of the sample holder. Thus regarding simple models, i.e. Maxwell’s model, the asymptotic part of viscosity can be determined with much better precision, and it is also of major interest as the longer-term behavior of the materials is usually of importance. This is defined by the reverse of the creep compliance slope, whereas ‘instant modulus’ is defined by an inverse of the linear intercept.

To emphasize again, these model-fit moduli cannot be directly compared to the moduli obtained in DMA frequency sweep, compression tests or SAOS rheology, since the type of deformation in creep is very different, and the deformation is much larger (up to 10%). Another drawback of fitting Burger’s model is that two parameters ( $E_1$  and  $\eta_1$ ) are heavily dependent on the fitting of  $E_2$ , which does not depend solely on the material response. However, in general, the application of DMA allows analysis of both dynamic and creep or relaxation tests in the same device with same specimens, which might not be possible for other techniques. If some other evidence of application of either model were available, creep data would provide valuable information in addition to dynamic modes to predict long-term behavior of the material.

It is noteworthy that no specific theoretical preferences between known linear viscoelastic models were imposed, neither fitting parameters obtained from any such model fitting could be allocated to some realistic material data. Thus, the fitted numerical results shown below should be kept in mind as fitting parameters or functions, with little relevance to ‘viscosity’ or ‘creep modulus’ [22, 23], even when formally they could be called as such. It is also rather common to apply fractional derivatives with Laplace transform to creep functions data to ensure more realistic approximation in 3D cases [24].

#### 3.4. Which technique best describes the system?

All three measuring techniques have proven to be feasible to evaluate the mechanical properties of hydrogel-BAG composites. However, they differ either in the optimal size of the sample, type of sample deformation (compression or shear), boundary conditions and constraints, or type of deformation excitation (steady state or dynamic). For example, pure shear



does not lead to volume changes, so it is not sensitive to variations in the Poisson ratio and bulk properties. Although all three techniques describe the mechanical properties of the hydrogel composites, they do not provide the same material property and cannot be directly connected. In general, there is no direct correlation between ‘quasi’-static compression moduli and the complex compression moduli, because types of deformation excitation are different, although one could logically expect that a more stiff material should have high modulus values exhibited in both methods.

Therefore, the trends and values of moduli for these three techniques can be compared according to the amount of BAG in the hydrogels composites versus control hydrogel (figure 10). The trend of reinforcement (logarithmic scale) is clearly seen from the initial pure hydrogel to the composite with 2 wt.% BAG (H1). With further addition of BAG the increase of moduli is not so prominent. It is also evident that the moduli determined by all three techniques are in the same order of magnitude.

By uniaxial compression and DMA, one can measure properties of samples of the same size and shape, which are made in advance. This is very useful, as it is important to know mechanical properties of scaffold materials that have been subjected to a different environment for longer times [25]. For example, it is common to perform testing of scaffolds for bone regeneration in simulated bodily fluids (SBF) to observe the formation of HA [26]. This can be measured by these two techniques, whereas shear rheology (SAOS) in a rheometer is not suitable for this as the samples have to be made in the rheometer and cannot be removed without damaging them.

Conversely, the shear rheology is very useful to study the gelation of the hydrogels. Since SAOS can be

used to measure polymer solutions, the onset and kinetics of gelation could be easily identified, and for different cooling rates, the apparent activation energy for gel formation can be estimated. In the best case, a hint about the different structures of the polymer in the solution, like the presence of a weak polymer network prior gelation, could be obtained. Such a weak polymer network prevents sedimentation and agglomeration of BAG particles, which is very desirable. It is noteworthy that some special DMA sample holders also allow measurement of the viscosity changes of fluid samples, whereas compression tests cannot be technically used for this.

Maximum load (or stress) or deformation before breaking of scaffold materials is a very important material property but is very rarely measured, because it is not easy to observe it. This was also confirmed by our experiments in uniaxial compression. The examined hydrogels do not exhibit any observable yield point or brittle fracture, but their network breaks seamlessly as it is masked by nonlinear and viscoelastic behavior [27].

Therefore, the following measuring procedure could be suggested for biomechanical characterization of such materials: instead of deformation controlled by an arbitrarily chosen strain rate, creep experiments at different applied stresses are useful to carry out first. This is physiologically more relevant because, when such a material is used as a replacement of a damaged human tissue, it is subjected to certain loads, which exert stress on the scaffold material. This results in deformation, which is not the same as during deformation of the material with a certain strain and measuring stress (relaxation or stress-strain test). This is a consequence of complex viscoelastic behavior of hydrogels, where stress- and strain-controlled experiments can give very different results [27].

The second set of experiments is suggested to be carried out under physiologically relevant conditions, such as 1 Hz frequency and small amplitude-controlled deformation, in dynamic mode. These measurements could mimic, for example, articular cartilage or other tissue at working conditions [25, 28, 29]. The side effects like swelling, or cyclic fatigue could be identified at an early stage. By using different equilibration forces, swelling as a change in the thickness of the sample can be promoted or suppressed, thus giving an option to experimentally determine swelling pressure, for which the measurements are usually rather cumbersome [30, 31].

#### 4. Conclusions

The primary goal of this work was to reliably describe the behavior of hydrogel-based composites for tissue engineering scaffolds during mechanical loading. The effect of bioactive glass (BAG) particles embedded in gellan gum (GG) hydrogel was observed. Three common techniques were used and compared, analyzing their advantages and limitations: monotonic uniaxial unconfined compression, small amplitude oscillatory shear (SAOS) rheology and dynamic mechanical analysis (DMA).

The uniaxial compression test resulted in very similar values for the elastic modulus as the other two techniques but was not able to provide any additional data. SAOS rheology, along with elastic modulus, also provided information on dissipative modulus. Both shear moduli were measured at different deformation frequencies, providing a material response in the relevant physiological frequency range. In addition, when measuring hydrogel properties, SAOS rheological analysis can also provide valuable information on temperature-induced gelation. The only limitation of rheological measurement is the low thickness of the sample that prevents measurements of the thick, scaffold-like samples. Further, the DMA provides elastic and dissipative moduli in the same frequency range as SAOS rheology, but in compression. Moreover, the point of failure of hydrogel composites can be observed in stress controlled mode i.e. creep test. Therefore, creep and small amplitude dynamic strain-controlled tests in DMA, are suggested as the best ways for the characterization of mechanical properties of hydrogel composites, whereas the SAOS rheology is more useful for studying the hydrogel's processing kinetics, as it does not induce volumetric changes even at very high strains.

Overall, the beneficial effect of bioactive glass nanoparticles on the elastic modulus of the GG-BAG composite hydrogel has been confirmed. By additions of 2 wt.% BAG particles, the Young's modulus of  $6.6 \pm 0.8$  kPa for GG hydrogel increased by two orders of magnitude (500–800 kPa), which is ascribed to  $\text{Ca}^{2+}$  ions released from BAG, while a larger

addition did not further reinforce the material. All the composite samples have an approximate  $G'/G'' \sim 10$  and a little frequency dependence, which indicates a self-standing elastic gel. The point of destruction, revealed by the linear viscoelastic region, significantly decreased by the addition of BAG particles, i.e. from 10% of shear strain for GG to only 0.3–1.0%.

#### Acknowledgments

This work has been funded by Slovenian Research Agency as a part of a PhD study of the first author, Mr Rok Kocen. Part of the work was performed within a short-term Scientific Mission (STSM reference number: COST-STSM-ECOST-STSM-MP1005-160215-054079) with the group at Aalto University Foundation and was covered by a COST Action MP1005 'From nano to macro biomaterials (design, processing, characterization, modelling) and applications to stem cell regenerative orthopaedic and dental medicine—NAMABIO'.

#### References

- [1] Sivashanmugam A, Arun Kumar R, Vishnu Priya M, Nair S V and Jayakumar R 2015 An overview of injectable polymeric hydrogels for tissue engineering *Eur. Polym. J.* **72** 543–65
- [2] El-Sherbiny I and Yacoub M 2013 Hydrogel scaffolds for tissue engineering: progress and challenges *Glob. Cardiol. Sci. Pract.* **2013** 316–42
- [3] O'Brien F J 2011 Biomaterials and scaffolds for tissue engineering *Mater. Today* **14** 88–95
- [4] Lichte P, Pape H C, Pufe T, Kobbe P and Fischer H 2011 Scaffolds for bone healing: concepts, materials and evidence *Injury* **42** 569–73
- [5] Jin Y, Kundu B, Cai Y, Kundu S C and Yao J 2015 Bio-inspired mineralization of hydroxyapatite in 3D silk fibroin hydrogel for bone tissue engineering *Colloids Surf. B* **134** 339–45
- [6] Gantar A et al 2014 Nanoparticulate bioactive-glass-reinforced gellan-gum hydrogels for bone-tissue engineering *Mater. Sci. Eng. C* **43** 27–36
- [7] Lv H et al 2015 Mechanism of regulation of stem cell differentiation by matrix stiffness *Stem. Cell Res. Ther.* **6** 103
- [8] Wen J H et al 2014 Interplay of matrix stiffness and protein tethering in stem cell differentiation *Nat. Mater.* **13** 979–87
- [9] Chaudhuri O et al 2016 Hydrogels with tunable stress relaxation regulate stem cell fate and activity *Nat. Mater.* **15** 326–34
- [10] Sasaki N 2012 Viscoelastic properties of biological materials *Ann. N.Y. Acad. Sci.* **99**–122
- [11] Cowin S C (ed) 2001 *Bone Mechanics Handbook* 2nd edn (Boca Raton, FL: CRC Press) ([https://doi.org/10.1016/S0021-9290\(01\)00251-2](https://doi.org/10.1016/S0021-9290(01)00251-2))
- [12] Hu Y and Suo Z 2012 Viscoelasticity and poroelasticity in elastomeric gels *Acta Mech. Solida Sin.* **25** 441–58
- [13] Hu Y, Zhao X, Vlassak J J and Suo Z 2010 Using indentation to characterize the poroelasticity of gels *Appl. Phys. Lett.* **96** 121904
- [14] Strange D G T, Fletcher T L, Tonsomboon K, Brawn H, Zhao X and Oyen M L 2013 Separating poroviscoelastic deformation mechanisms in hydrogels *Appl. Phys. Lett.* **102** 31913
- [15] Drnovšek N 2012 Development of coatings on Ti6Al4V alloy for new generation implants bone with improved osseointegration *Doctoral Thesis* Institute Jozef Stefan, Slovenia

- [16] Luczynski K W, Brynk T, Ostrowska B, Swieszkowski W, Reihnsner R and Hellmich C 2013 Consistent quasistatic and acoustic elasticity determination of poly-L-lactide-based rapid-prototyped tissue engineering scaffolds *J. Biomed. Mater. Res. A* **101** 138–44
- [17] Greene G W *et al* 2008 Changes in pore morphology and fluid transport in compressed articular cartilage and the implications for joint lubrication *Biomaterials* **29** 4455–62
- [18] Zuidema J M, Rivet C J, Gilbert R J and Morrison F A 2013 A protocol for rheological characterization of hydrogels for tissue engineering strategies *J. Biomed. Mater. Res. B* **00B** 1–11
- [19] Miyoshi E, Takaya T and Nishinari K 1996 Rheological and thermal studies of gel-sol transition in gellan gum aqueous solutions *Carbohydr. Polym.* **30** 109–19
- [20] Gulrez S K H, Al-Assaf S and G O 2011 Hydrogels: methods of preparation, characterisation and applications *Progress in Molecular and Environmental Bioengineering - From Analysis and Modeling to Technology Applications* (Rijeka: InTech) pp 117–51
- [21] Noda S *et al* 2008 Molecular structures of gellan gum imaged with atomic force microscopy in relation to the rheological behavior in aqueous systems: I. Gellan gum with various acyl contents in the presence and absence of potassium *Food Hydrocoll.* **22** 1148–59
- [22] Findley W N, Lai J S and Onaran K 1976 *Creep and Relaxation of Nonlinear Viscoelastic Materials with an Introduction to Linear Viscoelasticity* (Amsterdam: North-Holland) (<https://doi.org/10.1002/zamm.19780581113>)
- [23] Williams M L 1964 Structural analysis of viscoelastic materials *AIAA J.* **5** 785–98
- [24] Makris N 1997 Three-dimensional constitutive viscoelastic laws with fractional order time derivatives *J. Rheol.* **41** 1007
- [25] Gasik M 2014 New BEST—biomaterials enhanced simulation test *ALTEX Proc.* **3** 33–34 <http://www.altex.ch/ALTEX-Proceedings/Proceedings.98.html?iid=4>
- [26] Kokubo T and Takadama H 2006 How useful is SBF in predicting *in vivo* bone bioactivity? *Biomaterials* **27** 2907–15
- [27] Pollock J F and Healy K E 2010 Mechanical and swelling characterization of poly(N-isopropyl acrylamide -co- methoxy poly(ethylene glycol) methacrylate) sol-gels *Acta Biomater.* **6** 1307–18
- [28] van der Meulen M C H and Huiskes R 2002 Why mechanobiology? A survey article *J. Biomech.* **35** 401–14
- [29] Kisiday J *et al* 2002 Self-assembling peptide hydrogel fosters chondrocyte extracellular matrix production and cell division: Implications for cartilage tissue repair *Proc. Natl Acad. Sci.* **99** 9996–10001
- [30] Van Meerveld J, Molenaar M M, Huyghe J M and Baaijens F P T 2003 Analytical solution of compression, free swelling and electrical loading of saturated charged porous media *Transp. Porous Media* **50** 111–26
- [31] Kurnia J C, Birgersson E and Mujumdar A S 2011 Computational study of pH-sensitive hydrogel-based microfluidic flow controllers *J. Funct. Biomater.* **2** 195–212